Two-terminal resistance of quantum Hall devices

G. L. J. A. Rikken
Hochfeld-Magnetlabor, Max-Planck-Institut für Festkörperforschung, B.P. 166X, F-38042 Grenoble Cédex, France and Research Institute for Materials, University of Nijmegen, Toernooiveld, NL-6525 ED Nijmegen, The Netherlands

J. A. M. M. van Haaren
Research Institute for Materials, University of Nijmegen, Toernooiveld, NL-6525 ED Nijmegen, The Netherlands

W. van der Wel
Department of Applied Physics, Delft University of Technology, P.O. Box 5046, NL-2600 GA Delft, The Netherlands

A. P. van Gelder and H. van Kempen
Research Institute for Materials, University of Nijmegen, Toernooiveld, NL-6525 ED Nijmegen, The Netherlands

P. Wyder
Hochfeld-Magnetlabor, Max-Planck-Institut für Festkörperforschung, B.P. 166X, F-38042 Grenoble Cédex, France and Research Institute for Materials, University of Nijmegen, Toernooiveld, NL-6525 ED Nijmegen, The Netherlands

J. P. André
Laboratoire d'Electronique et de Physique Appliquée, F-94450 Limeil-Brevannes, France

K. Ploog
Max-Planck-Institut für Festkörperforschung, D-7000 Stuttgart 80, Federal Republic of Germany

G. Weimann
Forschungsinstitut der Deutschen Bundespost beim Fernmeldetechnischen Zentralamt, D-6100 Darmstadt, Federal Republic of Germany

(Received 31 August 1987)

An analytic solution of the current distribution in a two-dimensional electron gas (2D EG) near an abrupt variation in the conductance properties is given. This solution is shown to explain the approximate quantization of the two-terminal resistance of a 2D EG at values of h/ie^2. The difference between the two-terminal resistance and the Hall resistance is shown to be determined by an interplay of contact and 2D EG properties, and is argued to be of the order of 10^{-6} times the Hall resistance or less, for Au-Ge-Ni and Sn contacts. Measurements in agreement with this prediction are presented.

I. INTRODUCTION

To measure the dc-resistivity tensor components of a conductive slab accurately, one always uses a four-terminal method in order to eliminate contact effects (Fig. 1). With such a method, the two-dimensional electron gas (2D EG) in MOSFET's (Ref. 1) (metal-oxide–semiconductor field-effect transistors) and heterostructures[2] has been found to give an accurately quantized, four-terminal Hall resistance, whereas the longitudinal resistance vanished. (See Fig. 1 for definitions of these quantities and their magnetic field dependencies.) This quantum Hall effect is intensively studied for its fundamental implications and has found a wide application in metrology. It has also been shown that the quantum Hall effect yields a quantized resistance in a two-terminal measurement, i.e., measuring the voltage across the current source and drain contacts (Fig. 1). The accuracy of this quantization has been found to be quite high,[3,4] but no lower limit has been reported. Satisfactory explanations of this phenomenon, taking into account the interaction of the 2D EG with three-dimensional, metallic contacts have not yet been given. In this paper we will show that the potential distribution within a system that consists of a 2D EG between two metallic contact regions of arbitrary thickness can be calculated analytically. This is then used to estimate the accuracy of the quantization of the aforementioned two-terminal resistance. Furthermore, we present high-accuracy measurements of this quantity, which are found to be in agreement with the calculation.

This paper is organized as follows. In Sec. II previous experimental and theoretical work on the two-terminal resistance is discussed. It is shown that the analytic solu-

 ©1988 The American Physical Society

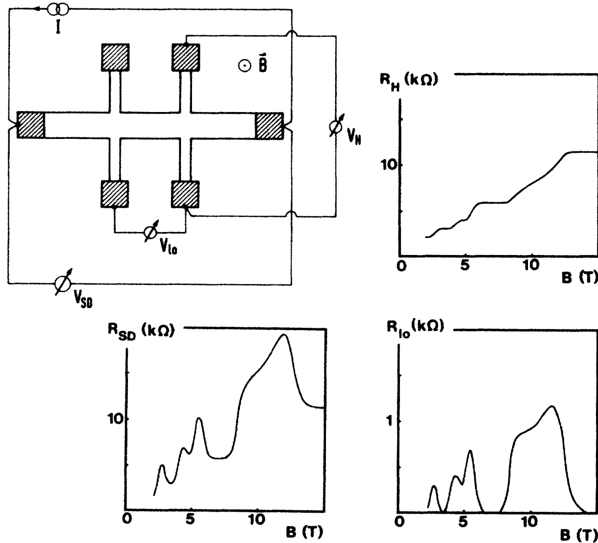

FIG. 1. Definition of resistances: the two-terminal resistance R_{SD} given by V_{SD}/I, the Hall resistance R_H by V_H/I, and the longitudinal resistance R_{lo} by V_{lo}/I, as well as their magnetic field dependencies for the case of a 2D EG between metallic contacts.

tion of the transport problem by Bruls and van Gelder[5-8] applies to this problem. Deviations of the two-terminal resistance with respect to the quantized Hall resistance are evaluated. In Sec. III measurements of the two-terminal resistance are presented and compared to the theory.

II. THEORY

Experiments on samples in the quantum Hall regime show that the two-terminal resistance R_{SD} equals the quantized Hall resistance within a measurement accuracy of 10^{-5} (Refs. 3 and 4). By making all kinds of interconnections between contacts on the same device, R_{SD} could be tailored to rational fractions of the quantized Hall resistance, and this elegantly proves that the two-terminal resistance is due to current redistributions at each interface between the 2D EG and a current-carrying contact.[3] The physical cause for such a redistribution is the large difference in Hall voltage for a 2D EG and a metallic slab: For Kirchoff's first law ($\oint \mathbf{E}\cdot dl = 0$) to be obeyed, the difference between the voltages across the interface along the two sides of the sample has to equal the Hall voltage difference. To achieve this, the current in the transition region will be displaced towards one side of the sample. The quantized Hall resistance has been shown to be equal to h/ie^2, where i is an integer, within the accuracy of 5×10^{-8} with which this quantity is known (Ref. 9). On one hand, the accuracy of the two-terminal resistance is surprising, as the current distribution is highly disturbed near the current contacts; on the other hand, a possibly significant deviation from the four-terminal Hall resistance remains to be investigated. Theoretical work up to now[10-14] has not given a satisfactory description. Rendell and Girvin[10] and Al'tshuler and Trunov,[11] considering short-circuiting contacts, calculate a relative deviation of the order of the difference of the Hall angle from $\pi/2$, which can be smaller than 10^{-10} under standard laboratory conditions.[15] Finite-resistivity contacts were very recently considered by Neudecker and Hoffmann with numerical methods,[12] but the magnitudes of the resistivities and Hall resistances in their analysis do not apply to the two-terminal resistance of a 2D EG in the quantum Hall regime between metallic contacts. Thouless[13] calculates the potential distribution in a quantum Hall device obtaining results similar to Refs. 10 and 11. He gives a correction due to the current injection in the contact material for two-dimensional contacts and an approximation of the correction for three-dimensional contacts. He finds that the dimension of the contact in the magnetic field direction is of minor importance for the dissipation near the contact–2D EG interface. Syphers and Stiles[14] experimentally find a dependence of this deviation on the contact-preparation method, which they attempt to explain with their heuristic interactive boundary model.

The electric field and current distribution in a long two-dimensional strip with two neighboring regions, which have different Hall resistances, have been calculated by Bate, Bell, and Beer[16] and by Bruls and van Gelder.[5-8] The exact, analytic solution of the transport problem in Ref. 5 has been shown to describe magnetoresistance data on pure aluminum at 4.2 K,[6,7] and on gallium arsenide at room temperature,[8] without the use of adjustable parameters. In those experiments the variations of the two-dimensional resistivity tensor were realized by varying the sample thickness of the three-dimensional samples. However, the analytic solution can be applied to variations in the Hall resistance that have been achieved by various mechanisms, including difference in sample thickness, difference in carrier concentration, or spatial gradient in the magnetic field. A solution to this transport problem can be found[5] if the following two conditions are fulfilled: First, the conduction in both regions is described by a resistivity tensor. Secondly, the current pattern far away from the interface must be homogeneous. Moreover, we assume, for mathematical convenience, that the transition length between both regions is small compared to the sample width. The calculation yields a magnetic-field-dependent current distribution which is inhomogeneous over a distance L along the strip on either side of the transition, where L is the width of the strip.

For the moment we will assume that for the case of a long strip of 2D EG between two metallic contact regions (e.g., standard Hall bar geometries) the above conditions are fulfilled; consequences of departures from these conditions will be discussed below. The two contact–2D EG transition regions can be treated as independent parts with a homogeneous current pattern in the intermediate region, since they are a distance much larger than $2L$ apart. From the boundary conditions it can be shown[16] that in the two independent parts the current pattern is symmetric around its interface. From these considerations and using methods of conformal mapping similar to those used in Refs. 10 and 11, one finds a current pattern

as illustrated in Fig. 2, where for $x \geq 0$ and $0 \leq y \leq L$ the current distribution is given by[5]

$$J_x(x,y) - iJ_y(x,y) = \frac{I}{L}\left[\tanh\left[\frac{\pi(x+iy)}{2L}\right]\right]^{2\phi/\pi-1}, \quad (1)$$

where I is the current, L the width of the Hall bar,

$$b = \left|\frac{\rho_{xy,c}-\rho_{xy,2D}}{\rho_{xx,c}+\rho_{xx,2D}}\right|, \quad (2)$$

and

$$\phi = \pi/2 - \arctan b \; . \quad (3)$$

The indices c and 2D refer to the contact and the 2D EG. We note that so far the contact has been treated as a two-dimensional, conducting region, and that the tensor elements in Eq. (2) are two-dimensional resistivities with the dimension of resistance. The translation of the three-dimensional resistivity tensor of the contacting material into the $\rho_{xx,c}$ and $\rho_{xy,c}$ values, which appear in Eq. (2), has been made by means of a division by an effective contact thickness, which will be discussed below. It can be shown that the results of Refs. 10 and 11 can be obtained as limiting cases of Eqs. (1)–(3) with $\rho_{xx,c}=0$ and $\rho_{xy,c}=0$.

In Fig. 2 we used $b=10^5$, which is a reasonable value for the interface between a 2D EG in the quantum Hall regime and a contact, as will be argued in our discussion of real contacts below. The current pattern is a function of a single parameter that measures both the difference between the regions and the magnetic field. The constrictions shown in Fig. 2 will manifest themselves in a two-terminal resistance R_{SD} (as defined in Fig. 1) through the dissipation associated with them. Neglecting the resistance of the part of the 2D EG with a homogeneous current pattern, we find, with the evaluated current pattern, for the source-drain resistance in Fig. 2,

$$R_{SD} = (\rho_{xx,c}+\rho_{xx,2D})\left[1+\frac{2}{\pi}\psi(\tfrac{1}{2})-\frac{1}{\pi}\psi\left[\frac{\phi}{\pi}\right]-\frac{1}{\pi}\psi\left[1-\frac{\phi}{\pi}\right]\right], \quad (4)$$

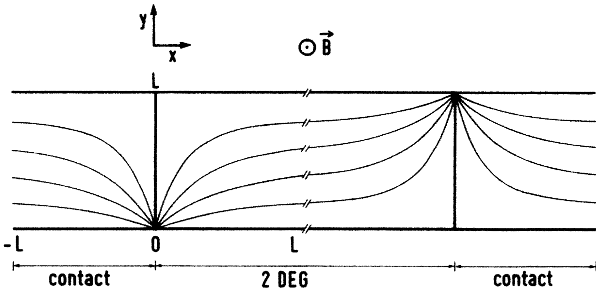

FIG. 2. Calculated current pattern across the contact–2D EG interfaces for $b=10^5$. The current pattern is homogeneous in the omitted part of the strip.

where ψ is the digamma function,[17] and ϕ is given by Eq. (3). Expanding the digamma function as a series of Riemann ζ functions yields

$$R_{SD} = |\rho_{xy,2D}-\rho_{xy,c}| + (\rho_{xx,c}+\rho_{xx,2D})\left[1-\frac{4}{\pi}\ln 2+\frac{2}{\pi}\frac{\phi}{\pi-\phi} + \frac{2}{\pi}\sum_{n=2}^{\infty}[\zeta(n)-1]\left[\frac{\phi}{\pi}\right]^{n-1}\right]. \quad (5)$$

For $b \gg 1$, which is the case for the experimental conditions considered below, Eq. (5) reduces to

$$R_{SD} = |\rho_{xy,2D}-\rho_{xy,c}| + (\rho_{xx,c}+\rho_{xx,2D})[0.12+O(1/b)] \; . \quad (6)$$

So in this model the two-terminal resistance is equal to the Hall resistance of the 2D EG, with corrections originating from the Hall resistance and the diagonal resistance of the contact. In most cases, $\rho_{xx,2D} \ll \rho_{xx,c}$, as follows from the discussion below.

We mentioned above that the resistivity tensor of the contact that is used in Eqs. (2)–(6) is given by the three-dimensional resistivity tensor of the contacting material divided by an effective contact thickness. This effective thickness is introduced by the averaging of the three-dimensional current density and electric field in the contact, over the coordinate along the magnetic field direction, after which a solvable two-dimensional transport problem remains. Details on this procedure can be found in Refs. 6 and 7. Only the parts in the three-dimensional contact through which a current is flowing, must be taken into account for this averaging. We will estimate this effective thickness for two commonly used—but in this respect inequivalent—types of contacts. For evaporated contacts the actual thickness t will be much smaller than the width of the 2D EG L (see Fig. 3). The three-dimensional current distribution will be homogeneous along the magnetic field direction at in-plane distances t from the contact–2D EG interface. Therefore the effective thickness will equal t. However, for alloyed metal dots (Fig. 4) the thickness t will be comparable to or larger than L. In that case the current will not be homogeneously distributed along the magnetic field direction at distances L from the interface. As the resistance associated with the constriction is located within distances L from the interface, one should take as the effective thickness of the contact the thickness of the current pattern at distances L from the interface. Due to the harmonic character of the potentials associated with this problem, this extent—and therefore the contact's effective thickness—is of the order L.

As Fig. 2 shows, the current is squeezed into one corner of the contact–2D EG interface, and the locally high current density will result in a breakdown of the quantized Hall effect.[18,19] Under standard experimental conditions with overall current densities in the 2D EG of 0.1–0.01 A/m, the calculated current density exceeds the

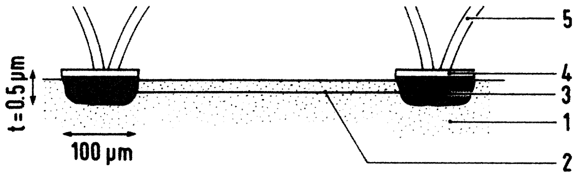

FIG. 3. Cross section of the contacts to the 2D EG: 1 denotes the heterostructure, 2 the 2D EG, 3 the alloyed contact, 4 the metallic overlayer, and 5 a lead. The effective thickness of the contact is 0.5 μm, the distance between the contacts is ~ 1 mm.

experimentally determined breakdown current density of 0.5 A/m (Ref. 18) in a region with the size of 10–1 % of the bar width. In this region, $\rho_{xx,2D}$ increases 5 orders of magnitude.[19] However, this hardly affects the parameter ϕ, which determines the current distribution, because ϕ is dominated by $\rho_{xy,2D}$ and $\rho_{xx,c}$, as will be shown below. Therefore, the current distribution of Eqs. (1)–(3) applies to the entire sample.

Now we will consider the properties of realistic, three-dimensional contacts to a 2D EG in GaAs-(Al,Ga)As heterojunctions in more detail, in order to estimate the corrections on the quantized Hall resistance that can be expected in a two-terminal resistance measurement. (The ideas will be applicable to the case of a 2D EG in a MOSFET as well.) The two most commonly applied contacts are the Au-Ge-Ni composite, which is widely used in commercial electronic devices, and pure tin. The latter is usually restricted to laboratory applications because, though simple to apply, it is not stable over long periods of device operation.

We will first focus on the Au-Ge-Ni contact. The alloyed contact consists of a mixture of alloys such as NiGe, NiAs, Ni_2AsGe, and Au_3Ga, of which the first three are most important in reducing the contact resistance.[20] It has been shown that these alloys are stoichiometric,[20] and although no data are available on their resistivities and carrier concentrations at cryogenic temperatures, it seems reasonable to take as an order-of-magnitude estimate the values for impure nickel, i.e., 10^{-8} Ω m and 10^{29} m^{-3}, respectively.[21] The thickness of the contact as seen by the 2D EG is of the order of 0.5 μm, being the thickness of the evaporated contact layers. Alloying times of the order of minutes are sufficient to let the alloys reach the 2D EG (typically 200 nm below the surface).

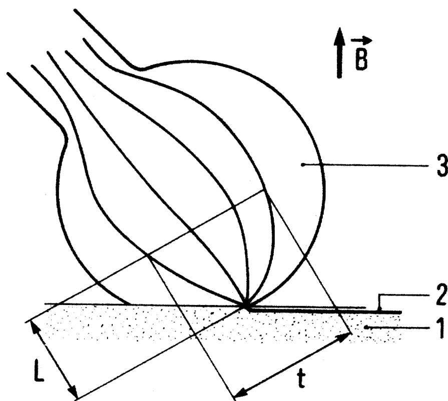

FIG. 4. Sketch of the current pattern in the Sn contact: 1 denotes the heterostructure, 2 the 2D EG, and 3 the Sn dot. The current flows through an elongated part of the dot, with an effective thickness $t \approx L \approx 100$ μm.

As the tin contact has limited commercial use, very little is known about the exact contact structure. A typical fabrication procedure is to alloy tin dots of less than 1 mm diameter in a reducing atmosphere at 400 °C for 4 min. Probably a mixture of SnAs and Sn_3As_2 alloys will be formed, with resistivities and carrier concentrations comparable with the alloys in the Au-Ge-Ni case.

In practical samples the contact areas are approximately square or circular, with dimensions of about 100 μm, and the current and voltage leads are positioned near the center of the contact. The transition region between contact and 2D EG is a ribbon of at most 0.5×0.5 μm^2 cross section, so the solution of Ref. 5 can be applied. The contact–2D EG geometry in practical samples may differ somewhat from the mathematically convenient form in Fig. 2, but as the main part of the dissipation occurs in a very small region near the interface, the expression in Eq. (6)—possibly with slightly altered numeric constants—will apply to practical contact–2D EG geometries. The same conclusion follows from considerations of inhomogeneities in the current pattern in the "bulk" of the 2D EG as observed by various workers,[22–25] because the constrictions will be dominated by the difference in properties of the contact and the 2D EG.

For the Au-Ge-Ni contact (0.5 μm thickness), one finds relative corrections to the quantized resistance h/ie^2 at the $i=2$ plateau due to the second, third, and fourth terms in Eq. (6) of about 10^{-8}, 2×10^{-7}, and 10^{-12}, respectively. The accuracy of the two-terminal resistance is therefore limited by an interplay of contact and 2D EG, and not by the finiteness of the ratio $\rho_{xy,2D}/\rho_{xx,2D}$.

For the tin contacts (100 μm effective thickness) one finds from Eq. (6), for the aforementioned corrections, 5×10^{-11}, 10^{-9}, and 5×10^{-14}, respectively.

III. EXPERIMENTAL RESULTS AND DISCUSSION

The measurements were made with four samples, whose properties are listed in Table I. Three samples were provided with Au-Ge-Ni contacts by vapor deposition and subsequent alloying. The resistance of the current leads was measured separately and corrected for $(\sim 10^{-6})$. Sample 4 was provided with small Sn dots, which were alloyed into the 2D EG. In this sample the two-terminal resistance R_{SD} was measured directly at the juncture of the current leads to the sample.

The resistance R_{SD} was compared with the Hall resistance R_H by means of the potentiometric resistance comparator at the Van Swinden Laboratories (VSL) of the Dutch National Standards Institute[26] with a resolution of better than 3×10^{-8}. The measurement of the current leads (for samples 1–3) adds an uncertainty of 10^{-7}. The data were taken at a temperature of 1.2 K so as to minimize $\rho_{xx,2D}$. A complication is the possible inhomogeneity of the samples: The magnetic field is chosen such that

TABLE I. Sample properties. MOCVD denotes metallic-organic chemical-vapor deposition, MBE molecular-beam epitaxy.

Sample	Growth technique	Electron density (10^{15} m^{-2})	Mobility (m^2/V s)	Contacts
1	MOCVD	3.6	10	Au-Ge-Ni
2	MOCVD	4.0	15	Au-Ge-Ni
3	MBE	3.7	13.5	Au-Ge-Ni
4	MBE	2.5	60	Sn

$\rho_{xx,2D}$ as measured in the middle of the channel is minimal. Owing to the variations of electron density along the channel, some parts of the sample might be well off the $\rho_{xx,2D}$ minimum. Then the resulting (nonvanishing) longitudinal resistance of the 2D EG that connects both contact regions might contribute significantly to R_{SD}. To confirm the absence of this, it was checked that the channel current was low enough so that no current dependence was detectable, neither in the quantized Hall resistance nor in the two-terminal resistance. As $\rho_{xx,2D}$ is also strongly current dependent,[27] this proves that it does not contribute significantly to the observed resistances. Only in sample 2 do both the $i=4$ and $i=2$ plateaus have sufficiently low $\rho_{xx,2D}$ to ensure that the contribution of the longitudinal resistance to R_{SD} is negligible.

Table II gives the results. For the thin Au-Ge-Ni contacts the values of $R_{SD}-R_H$ are of the predicted order of magnitude. For sample 2, $R_{SD}-R_H$ is independent of the plateau index i, in agreement with our model. For the case of the Sn contact the predicted difference is smaller than the instrumental resolution. This is in reasonable agreement with the experimental result. It should be noted that the given uncertainty is merely a 1σ estimate. To confirm that the small value of $R_{SD}-R_H$ in sample 4 is caused by the larger thickness of the contact, we spread a Sn layer, with an estimated thickness of ~ 10 μm, on the Au-toplayer of the Au-Ge-Ni contacts of sample 3, by melting small pieces of Sn on the contacts. The sample was heated to a temperature just above the melting point of Sn for a short time to minimize damage to the underlying Au-Ge-Ni contact. The value for $(R_{SD}-R_H)/R_H$ was found to be 7×10^{-8} for these thicker contacts.

As an alternative explanation for the observed difference between R_{SD} and R_H, one could think of the metal-semiconductor contact resistance. The magnitude of such a resistance in the case of a metal–2D EG contact is unknown. One would expect, however, that such a mechanism would give approximately the same results for $R_{SD}-R_H$ for the Sn and Au-Ge-Ni contacts. This mechanism would not explain the dependence of $R_{SD}-R_H$ on the thickness of the metal contact that is indicated here.

TABLE II. Relative difference between the two-terminal resistance (R_{SD}) and the four-terminal Hall resistance (R_H) at the plateaus. The indicated uncertainties are 1σ estimates.

Sample	Plateau index i	Current (μA)	$(R_{SD}-R_H)/R_H$ (10^{-6})
1	2	9–27	0.8±0.1
2	2	9–27	0.4±0.1
2	4	9–27	0.8±0.1
3	2	9–18	1.2±0.1
4	2	4.5	0.05±0.03

Figure 5 shows the results of this work as well as previously published results on this subject. A striking consequence of the result summarized in Eq. (6) is that R_{SD} could, in principle, be smaller than R_H if the contact material has a large $\rho_{xy,c}$. The physical cause for this rather unexpected[28] result can be seen from Fig. 2: In both contact regions there is a current component perpendicular to the long axis, which causes a (Hall) voltage along the long axis that opposes the voltage drop within the 2D EG. In this argument it is essential that V_{SD} is measured with potential leads that have their connections to the contact on the 2D EG within the magnetic field region (see Fig. 1). A different situation occurs if V_{SD} is probed on the leads for current supply at such distances of the 2D EG that the potential difference is registered between points that lie outside the magnetic field. In that case $\rho_{xy,c}=0$ at the measurement positions and the negative contribution to $R_{SD}-R_H$ will vanish. However, the analysis of realistic contacts given above shows that even in the measurement configuration of Fig. 1 a negative value for $R_{SD}-R_H$ will not be readily observable.

Now that measurements support our model, we would like to finish up by pointing out how $R_{SD}-R_H$ can be measured directly in a *three-probe configuration* on a sample that is in the quantized regime. We propose to apply the current through the source and drain contacts as in Fig. 1, and to measure the voltage between the source contact and a Hall probe. It follows from our calculations and from Fig. 2 that this value is approximately

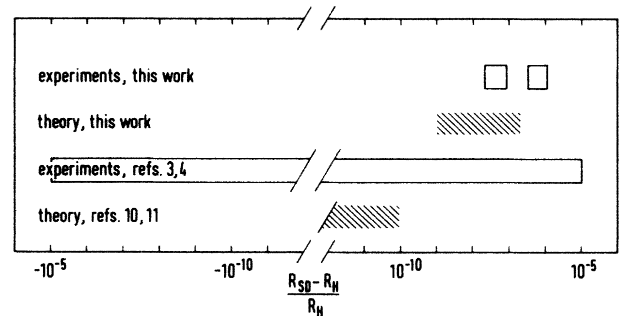

FIG. 5. The relative difference of the two-terminal resistance R_{SD} and the Hall resistance R_H according to previous theoretical and experimental work and the present work. It was reported that R_{SD} equals R_H experimentally within the measurement accuracy of 10^{-5} (Refs. 3 and 4). The published theories, considering idealized short-circuiting contacts, predict differences of 10^{-10} or less (Refs. 10 and 11). Our model for realistic contacts predicts larger differences. Our measurements with thin evaporated contacts (the larger values) and with thick alloyed contacts (the lower ones) show a significant difference between R_{SD} and R_H, which can be explained with our model.

equal to R_H for Hall probes on one side of the sample. However, for the probes on the opposite side, the measurement yields $(R_{SD}-R_H)/2$ directly. This way of determining $R_{SD}-R_H$ requires only a nanovoltmeter and a μA-current source, instead of a high-resolution resistance comparator. This can be applied for measuring properties of the contact via Eq. (6), taking advantage of the well-defined resistive properties of a 2D EG in the quantized regime.

In summary, we have presented a theoretical model for $R_{SD}-R_H$ and order-of-magnitude calculations of this quantity for commonly used contact methods: alloyed Sn dots and evaporated Au-Ge-Ni contacts. Furthermore, we have presented experimental results in agreement with our calculations. Our experiments show that thin Au-Ge-Ni contacts produce a measurable difference between R_{SD} and R_H in the quantized regime. In order to make more affirmative statements, the exact properties of the alloys constituting the contact regions have to be known more accurately. Conversely, one may start from our model and then the two-terminal resistance, or the results of a newly proposed three-probe measurement, may yield information on the contact properties.

ACKNOWLEDGMENTS

We are grateful to Dr. G.J.C.L. Bruls and Dr. J.C. Maan for critical readings of the manuscript. Part of this work was supported by the Stichting voor Fundamenteel Onderzoek der Materie (FOM), with the financial support of the Nederlandse Organisatie voor Zuiver Wetenschappelijk Onderzoek (ZWO), and by the Stichting voor Technische Wetenschappen (STW).

[1]K. von Klitzing, G. Dorda, and M. Pepper, Phys. Rev. Lett. **45**, 494 (1980).

[2]D. C. Tsui and A. C. Gossard, Appl. Phys. Lett. **38**, 550 (1981).

[3]F. F. Fang and P. J. Stiles, Phys. Rev. B **27**, 6487 (1983); **29**, 3749 (1984).

[4]T. G. Powell, C. C. Dean, and M. Pepper, J. Phys. C **17**, L359 (1984).

[5]A. P. van Gelder (unpublished). See also Refs. 6–8.

[6]G.J.C.L. Bruls, J. Bass, A. P. van Gelder, H. van Kempen, and P. Wyder, Phys. Rev. Lett. **46**, 553 (1981).

[7]G.J.C.L. Bruls, J. Bass, A. P. van Gelder, H. van Kempen, and P. Wyder, Phys. Rev. B **32**, 1927 (1985).

[8]J.A.M.M. van Haaren, Ph.D. thesis, University of Nijmegen, 1988 (unpublished).

[9]E. Richard Cohen and Barry N. Taylor, Europhys. News **18**, 65 (1987) (unpublished).

[10]R. W. Rendell and S. M. Girvin, Phys. Rev. B **23**, 6610 (1981).

[11]E. L. Al'tshuler and N. N. Trunov, Pis'ma Zh. Eksp. Teor. Fiz. **42**, 99 (1985) [JETP Lett. **42**, 119 (1985)].

[12]B. Neudecker and K. H. Hoffmann, Solid State Commun. **62**, 135 (1987).

[13]D. J. Thouless, J. Phys. C **18**, 6211 (1985).

[14]D. A. Syphers and P. J. Stiles, Phys. Rev. B **32**, 6620 (1985).

[15]D. C. Tsui, H. L. Störmer, and A. C. Gossard, Phys. Rev. B **25**, 1405 (1982).

[16]R. T. Bate, J. C. Bell, and A. C. Beer, J. Appl. Phys. **32**, 806 (1963).

[17]*Handbook of Mathematical Functions,* edited by M. Abramowitz and I. A. Stegun (Dover, New York, 1965), p. 258.

[18]G. Ebert, K. von Klitzing, K. Ploog, and G. Weimann, J. Phys. C **16**, 5441 (1983).

[19]S. Komiyama, T. Takamasu, S. Hiyamizu, and S. Sasa, Solid State Commun. **54**, 479 (1985).

[20]T. S. Kuan, P. E. Batson, T. N. Jackson, H. Rupprecht, and E. L. Wilkie, J. Appl. Phys. **54**, 6952 (1983).

[21]J. Hugel, J. Phys. F **3**, 1723 (1973).

[22]E. K. Sichel, M. L. Knowles, and H. H. Sample, J. Phys. C **19**, 5695 (1986).

[23]G. Ebert, K. von Klitzing, and G. Weimann, J. Phys. C **18**, L257 (1985).

[24]H. Z. Zheng, D. C. Tsui, and Albert M. Chang, Phys. Rev. B **32**, 5506 (1985).

[25]R. Woltjer, R. Eppenga, J. Mooren, C. E. Timmering, and J. P. André, Europhys. Lett. **2**, 149 (1986).

[26]W. van der Wel, C. J. P. M. Harmans, R. Kaarls, and J. E. Mooij, IEEE Trans. Instrum. Meas. **IM-34**, 314 (1985).

[27]W. van der Wel, C.J.P.M. Harmans, and J. E. Mooij, Surf. Sci. **170**, 226 (1986).

[28]K. von Klitzing (private communication).